UCRL-ID-118658

Noble Gas Isotope Measurements for Spent Nuclear Fuel Reprocessing

IAEA Task 90/0A211 Interim Report

G. Bryant Hudson
Nuclear Chemistry Division

February 17, 1993

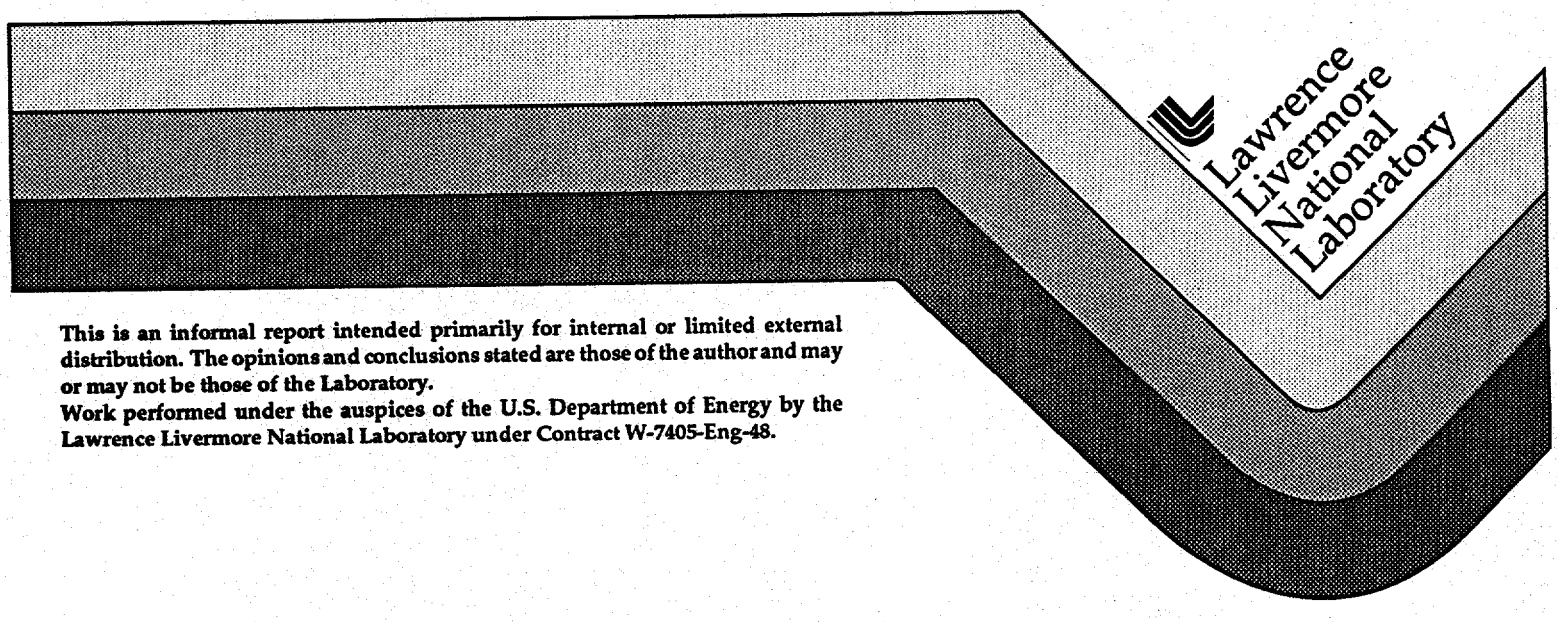

Work performed under the auspices of the U.S. Department of Energy by the Lawrence Livermore National Laboratory under Contract W-7405-Eng-48.

DISCLAIMER

Portions of this document may be illegible in electronic image products. Images are produced from the best available original document.

Introduction

The nuclear fission of actinides in reactor fuel produces large quantities of Kr and Xe as fission products. Because of the high levels of fission Kr and Xe, sample collection and analysis of noble gases for spent fuel diagnostic measurements is a simple, straight-forward technique.

In modern reprocessing plants with continuous dissolvers, it will not be possible to use traditional methods for isolating input batches of fuel. This study investigates the feasibility of using noble gas isotope abundance measurements (isotope correlation techniques - ICT) to solve safeguards requirements. Noble gas measurements might be able to provide an independent analysis of Pu contained within dissolves fuel, on an individual fuel assembly basis.

The isotopic composition of Kr and Xe in spent fuel reflects both the composition (isotope abundance ratios) of the fission products and the effects of neutron capture on those fission products.

We have reviewed the available literature for noble gas analyses of spent reactor fuel. While references are made to noble gas isotope correlations over the last 20 years, we have found little if any detailed analysis of large data sets. It seems possible that such analyses exist and we have not uncovered them. The literature search did find several useful reports (refs. 1-5). Of these papers, one is particularly useful for evaluating noble gas isotopic compositions. The 'Benchmark' paper (1) contains 54 Kr and 56 Xe isotopic composition analyses for 4 different reactors with a variety of fuel enrichment factors. Burnup ranges from 8000 to 37000 MWd/tU. Besides the noble gas measurements, a variety of other measurements are reported (actinides and fission products). While noble gas data is given in this report it is not analyzed in the report. The second reference, 'The Isotope Correlation Experiment', provides Kr and Xe data for 10 samples from the Obrigheim reactor with burnup ranging from 27 to 32 GWd/tU. The third reference, 'Gaseous Isotope Correlations Technique For Safeguards at Reprocessing Facilities', provides an excellent general discussion of the problem and shows calculational estimates of the effects of initial ^{235}U and enrichment and the neutron energy spectrum. The fourth and fifth reference provide data on Kr and Xe released during the opening, chopping and dissolution of 5 irradiated fuel rods with a burnup of 31 GWd/tU from the Borssele reactor. The loss and redistribution of Kr and Xe from the fuel during irradiation is an important issue for the noble gas isotope correlation technique.

GH

Data Review

Most of the data comes from the dissolution of individual fuel rods. In all cases the rods were chopped into pieces before being dissolved. The gases released during chopping were not collected. One study (4,5) collected the noble gases released during opening and chopping. The data show that between 2 and 6% of the total Kr and Xe was lost during opening of the cladding and the chopping of the fuel before dissolution.

In all data sets, the noble gases released in the dissolution process are transported to a cold trap in a helium stream. Isotopic analysis was done with static noble gas mass spectrometry. We would expect few problems with this method and the absolute accuracy of the isotope ratios measurements should be much better than 1%. The observed shifts in the Kr and Xe isotopic ratios are large compared to the analytical uncertainties.

Table 1. summarizes relevant data from (refs. 1,2,5). Generally, we note that the burnup as determined by Nd isotopes agrees well with non destructive measurements of $^{134}Cs/^{137}Cs$. No data are available for ^{130}Xe and ^{82}Kr in (1,2). The isotopes of greatest interest are ^{83}Kr, ^{84}Kr and ^{86}Kr for Kr and ^{131}Xe, ^{132}Xe and ^{134}Xe for Xe. The abundance of ^{136}Xe is complicated by the large neutron cross section of ^{135}Xe (^{135}Xe half-life = 9 hr). A large part of the ^{135}Xe is converted to ^{136}Xe by neutron capture.

The isotopes ^{83}Kr and ^{131}Xe have large neutron absorption cross sections and a significant fraction of these atoms are converted to ^{84}Kr and ^{132}Xe . The other isotopes have small neutron absorption cross sections, especially ^{86}Kr.

We want to look at the internal consistancy of the data by looking for quantities which should not vary much. The sum of ^{83}Kr and ^{84}Kr is relatively insensitive to neutron exposure. There are small gains because of neutron capture by ^{82}Kr and there are small losses because of neutron capture by ^{84}Kr. The net effect is small and positive (2-3% at 30GWd/tU). The same is true for ^{131}Xe and ^{132}Xe except the sum should vary even less. Thus, if we examine a graph of $(^{131}Xe+^{132}Xe)/^{134}Xe$ versus $(^{83}Kr+^{84}Kr)/^{86}Kr$, we should see all analyses being similar. The small differences coming from the differences in the ratio of ^{235}U fission to ^{239}Pu fission (also ^{238}U fissions), with high burnup samples having more ^{239}Pu fissions. In fig 1. we see that much of the data lie near a trend given by the ORIGEN 2 calculation (6). We also notice some important deviations. The Obrighiem data from (2) has $(^{83}Kr+^{84}Kr)/^{86}Kr$ significantly greater than the

other data and what was expected based on known fission yields and neutron cross sections. No explanation for this large deviation has been found and this represents an unresolved problem. The effect is about a factor of 50 greater than stated experimental uncertainties. Also, there are two other extreme values for Obrigheim from (1). These observation raise some important concerns about the data, at least for the Obrigheim data from (2) and the two Obrigheim samples from (1). It is tempting to suggest that the data for the two samples from (1) have typographic errors.

The ratios of $^{84}Kr/^{83}Kr$ and $^{132}Xe/^{131}Xe$ are sensitive to neutron capture and will increase with increasing exposure. We can examine the correlation of the ratios with burnup as measured by Nd isotopes in figs. 2 and 3. The ratios increase with burnup as expected, however there are some considerable variations. Tables 2 and 3 give the deviations about a regression line characteristic of most of the data. There are important deviations from the simple correlation for both isotopes. Even if we exclude 20% of the data, the typical deviation is still about 10%. Some variations appear in both figs 2 and 3. We can look at the graph of $^{84}Kr/^{83}Kr$ versus $^{132}Xe/^{131}Xe$ (fig. 4) to see if the trend is simpler. If Kr and Xe were migrating to regions of lower temperature, they might disagree with Nd while Kr and Xe agreed on a different (and wrong) neutron fluence. However, we see that fig. 4 shows considerable scatter from a simple linear trend also.

The lack of a simple correlation is partly because of the types of samples included. These samples reflect the variability of being from different reactors and in a variety of positions. If we examine the relevant neutron cross sections we see that variations in the neutron energy spectrum will have important effects, especially for ^{131}Xe neutron capture. It is important to look at the data in a way that considers both the initial enrichment of the uranium fuel and the neutron energy spectrum that the sample experienced.

A simple model

To better use the Kr and Xe data, we need a model to account for the gross effects of fuel enrichment and neutron spectral changes. What we seek to model is not the operation of a nuclear reactor, but rather, the mix of reactions that might occur because of exposing uranium to neutrons. The model begins with one metric ton of uranium (10^6 grams). The amount of ^{235}U is specified. Neutrons are modeled in two groups. The first group uses thermal cross sections and the second group uses resonance integral cross sections. The total neutron fluence for a single step is specified (usually about 10^{19} n/cm^2). The calculation consists of 500 steps. The capture and fission cross

sections are given for both groups of neutrons. We use standard literature values (7) for the cross sections and fission yields except ^{238}U. For ^{238}U, the infinite dilution resonance integral is inappropriate because of the high number density of ^{238}U atoms. This work uses a value of 15 barns for the ^{238}U resonance integral cross section for all samples. The fission of ^{238}U is neglected. The chain fission yields to the Kr and Xe isotopes are taken to be instantaneous.

This is a simple model and the point is to show how multiple isotope measurements can constrain a parametrized model. The adjustable parameter in the calculation is the division of neutrons between the two energy groups. Figure 5 show the trajectory of a calculation for a specific burnup and neutron spectrum. The trajectory shows the evolution of the Kr and Xe ratios on successive exposures to neutrons. The spectral variable is adjusted to make the trajectory to pass through a given point. The fuel burnup is calculated by matching the observed Kr and Xe ratios . We can do this for each point and calculate a burnup value (MWd/tU) based on the number of fission reactions that occur in the model. The results of these calculations gives burnup up measurements which show a linear correlation with Nd based burnup values but the simple model is systematically low in predicting burnup. If we apply a linear calibration to the Kr, Xe derived burnup values we can bring the values into better agreement. The transformation applied is (MWd/tU) scaled = 1.5 * (MWd/tU) cal -5000. This normalization could have been better obtained by directly adjusting the neutron capture cross sections.

The results are summarized in figure 6 and table 4. To see how the model predicts Pu, fig. 7 shows the comparison between measured ^{239}Pu and ^{239}Pu predicted by the model that match the Kr and Xe data. Generally, we see agreement between the model and measurement (however both Obrigheim sets were not included because of their extreme behavior in figs 1,2,3). Despite the modest improvement over the correlations in figs. 2 and 3, the data are unable to reliably predict burnup or Pu with better than 10% accuracy.

There are several possibilities for this situation. The data may have problems. The typical accuracy for Kr and Xe isotopic measurements is about 0.1% to 0.2% for the major isotopes. The effects we see are about 10%, thus we need to invoke shifts of 50 standard deviations which seems unlikely. It difficult to imagine how noble gas mass spectrometry could produce a 5% error in a major isotope ratio, yet we observe some irregularities in fig. 1 which look like Kr measurement problems.

Another possibility is that the modeling is not detailed enough. Surely, the simple model considered here has its failings, particularly the adoption of 15 barns as the ^{238}U resonance

integral for all cases is a weakness. However, it is important to observe that the deviations from the simple correlations are complex, much of the variability happens within data sets from single reactors. The isotope correlations are not significantly improved by considering just one reactor at a time. However, it is useful to note the effects of averaging. In the 'Isotope Correlation Experiment' (2), when then total inventory is calculated the conclusions agree with other determination within a few percent, although individual data points differ by over 20%. By deleting 2 of the ten points (as done in ref. 2), then individual point determinations vary about 10%. So while better modeling may make more improvements than seen here with our very simple model, clearly such modeling will require fairly detailed descriptions of the irradiation history of each fuel assembly examined.

It appears likely that redistribution of fission Kr and Xe within the fuel rod sets basic limits on the potential precision of the Kr and Xe isotope correlations. It is well-known that Kr and Xe fission products migrate from the fuel. Reactor fuel rods typically include a plenum volume at the rod ends to accommodate these gaseous fission products (8). This effect presumably is more of a problem at higher burnup where the fuel has been either hotter or hot for a longer time. Our hypothesis is that a part (maybe half) of the disagreements between Kr and Xe derived burnup and Nd derived burnup comes from Kr and Xe redistribution.

Kr and Xe redistribution during irradiation

Krypton and xenon are volatile elements and their redistribution within fuel rods is well-known. The thermal conditions experienced by the fuel are quite sever. Central temperatures easily exceed 1200 C for months to years. We can compare these conditions to the retention properties of Kr and Xe in solids. While there is much doubt in assigning diffusion coefficients and activation energies to specific fuel materials, we known some about the retention properties of Kr and Xe in a variety of oxides and silicates from many studies of naturally occuring noble gases in solids. At a temperatures above 1200 C, most silicates and oxides loose significant amounts of Kr and Xe (despite the mechanism that trapped the gas in the solid), within only minutes to hours of heating.

If several percent of the fission Kr and Xe routinely escapes to the fuel rod ends, then how does this affect the remaining gas? It depends on how this gas interacts with the gas remaining in the fuel. For a steady leak from a homogeneous reservoir, the 4% loss corresponds to less than a 1% shift in the $^{132}Xe/^{131}Xe$ observed from dissolved the fuel. If the gas being lost represents an independent reservoir, then there is no shift in the composition of the retained gas. Gas loss is probably not a serious problem.

A greater concern comes from radial redistribution of Kr and Xe within the fuel. Because of the large radial temperature gradient in the fuel, it is possible that a significant part of the Kr and Xe might migrate to the outer, cooler regions of the fuel rod. The effect of this redistribution depends on the neutron fluence gradient across the fuel rod. Also, it depends on how uniformly the redistribution process operates. To the extent to redistribution varies from one fuel rod to the next is critical to the precision with which burnup and associated parameters can be determined.

The data from ref. 5 provide some information. Figure 8 shows a graph of $^{84}Kr/^{83}Kr$ versus $^{132}Xe/^{131}Xe$ for the data from ref. 5. All 5 rods behave quite similarly (burnup ranges from 31 to 32 GWd/tU as measured by ^{148}Nd). The gas released from dissolving the rods indicate as burnup of about 33 GWd/tU (from $^{132}Xe/^{131}Xe$ ratio). The gas released during the irradition into the fuel rod gas plenum shows a lower apparent burnup (about 23 GWd/tU based on Xe). The gas released on chopping shows a higher apparent burnup (about 41 GWd/tU based on Xe). The low value for the gas released during the irradiation is reasonable since space is provided in a plenum volume at the fuel rod ends to accommodate fission gases. The neutron flux is lower at the ends of the rods. The higher value associated with chopping shows there is a reservoir in the rod that received a higher than average neutron fluence.

This issue can be studied with noble gas mass spectrometry using small samples. A thin disk, cut from a fuel rod could be dissected to measure the radial profile of fission Kr and Xe. We have the facilities at LLNL to conduct such experiments.

Another obvious feature of fig. 8 is the distribution of $^{132}Xe/^{131}Xe$ values versus the distribution of the $^{84}Kr/^{83}Kr$ values. The Xe measurements group tightly in the three sets, the Kr measurements scatter more than the Xe measurements. There is no obvious cause for this. This is much like the case in fig. 1 for the data from ref. 2. When we consider both fig.1 and fig. 8 and the fact there is greater scatter in the $^{84}Kr/^{83}Kr$ vs. burnup correlation than for the Xe case, we should seriously consider than there is some unknown problem with the Kr data. But, the tight clumping of the Xe ratio s suggest that each of the rods behaved very similarly, which is a desirable feature.

Total isotope dilution techniques

The redistribution of fission Kr and Xe possibly limits the usefulness of these neutron capture burnup monitors. Neutron capture is not the only monitor of burnup, indeed it is an indirect measure. If we consider the fission produced isotopes of ^{86}Kr and ^{134}Xe, we notice that neutron capture barely affects their abundances. So if we could measure the total number of atoms of ^{86}Kr or ^{134}Xe produced by fission, we could directly determine the number of fissions associated with the sample with almost no model dependence. The lack of model dependence comes from that fact that the fission product ratios of ^{235}U and ^{239}Pu are similar. Such an isotope dilution measurement would be either too difficult or costly for most fission products, but for the noble gases, isotopically enriched rare isotopes like ^{124}Xe are inexpensive ($100/cm^{3}STP) and can potentially serve as tracers on a plant scale.

If we have a process gas stream at 150 m^3/hr of air, then we need to add 0.14 cm^3STP ^{124}Xe/hr to double the ^{124}Xe present in the stream. We can measure the tracer ^{124}Xe to 1% accuracy at this level, if we can use ^{126}Xe or ^{128}Xe as a monitor of the atmospheric Xe present (i.e. there must be no important nuclear source of these isotopes). This tracer addition rate corresponds to a tracer cost of $14/hr, modest compared to analysis costs. A comparable ^{78}Kr tracer would cost about $100/hr. For a ^{78}Kr tracer, we would hope to use ^{80}Kr as an air-Kr monitor.

In the best situation, sample dissolution would happen such that we could completely mix the tracer with the sample. This is probably not practical. Complete mixing might not be needed. We might be able to use the noble gas tracers in a secondary fashion. Periodic releases of noble gas tracers into the flow could calibrate the efficiency of the sampling system. The calibration would consist of releasing a known quantity of tracer and seeing what fraction was collected in the sampling operation. We measure total gas flow and noble gas concentrations to get the total amounts of ^{86}Kr and ^{134}Xe. The separation of chopping and dissolution in a plant setting is a potential problem since opening and chopping of the fuel is expected to release several percent of the total fission gas. Since this method depends on measuring the total number of noble gas fission products so it is necessary to include the gases released in chopping.

From an analytical measurement view, the greatest challenge comes in measuring the tracer in the presence of a large fission component. The ratio of ^{124}Xe to ^{136}Xe will be about 10^{-6}. This is within the known capability of noble gas mass spectrometry, but it imposes a greater burden for the mass spectrometry lab compared to simply measuring the fission Kr and Xe isotopic

compositions. With an isotope ratio this large, the mass spectrometer needs more than one detector to deal with the dynamic range. Standard practice is to use a faraday cup for the large ion beams and an electron multiplier for the smaller beams. The other major consideration comes from beam scattering. The large adjacent masses must not contribute significantly to the signal of the small beam. The low scattering rate requires that the size of the mass spectrometer must be fairly large (a radius of curvature of 50 cm for a single sector magnetic field mass spectrometer).

The ultimate accuracy of this method is probably a few percent. The errors would come from the following sources: the uncertainty in the total gas flow rate (1-2%), the uncertainty in the isotope ratio measurements (1-2%), uncertainty in the fission yield, especially the split between ^{235}U and ^{239}Pu fissions (1-2%). The total isotope dilution approach does not directly give details about Pu production. The Pu production would need to be modeled just as in any isotope correlation technique, however measurements of $^{132}Xe/^{131}Xe$ and $^{84}Kr/^{83}Kr$ would provide guidance in modeling and improve the prediction of Pu isotope abundances.

Another potential problem is suggested by data from ref. 5. This work reports a few measurements of ^{82}Kr, ^{128}Xe and ^{130}Xe. The values measured for ^{128}Xe and ^{130}Xe are considerably higher than that predicted by calculation. This suggests that it may be difficult to find an isotope of Kr or Xe that can be used to monitor air Kr and Xe present in the sample. The contribution for air derived ^{78}Kr and ^{124}Xe need to be measurable if these are to be useful tracers.

Sample collection

Since nuclear fission is such a strong source of Kr and Xe, instrumental sensitivity is not a major issue. For typical static noble gas mass spectrometry (i.e. the sample is contained statically within the mass spectrometer during analysis), the sample size is limited by the pressure in the mass spectrometer (pressures less than about 1×10^{-7} torr). A typical big (optimal) sample is about 10^{10} atoms of either Kr or Xe.

The size of the required gas volume is small. For concentrations between 0.01% and 1% Kr or Xe, we only need only a small fraction of 1 cm3STP for analysis by static noble gas mass spectrometry. Because the required sample is small and not especially radioactive, it is easy to ship samples by express mail. The biggest problem with this approach is the number of samples that should be measured. Probably collecting a sample every five minutes would be adequate. While the samples are small, it could be much work to keep track of such large numbers of samples.

A more desirable technique would be to do on-line noble gas mass spectrometry. A unique feature for on-line mass spectrometry is the presence of ^{85}Kr which can be simultaneously be measured by gamma ray spectrometry adding an important cross-calibration feature for the mass spectrometer and the gamma ray spectrometer. For the measurement of only major fission products of Kr and Xe, a commercial quadrupole mass spectrometer should be adequate. Measurements uncertainties of 1-2% for major noble gas isotope ratios should be possible for concentrations as low as 0.01% Kr or Xe. We have recently done experiments with a small commercial GQMS (gas quadrupole mass spectrometer) measuring Kr and Xe (4% concentration each in air). We can continuously measure the major isotope ratios to 1% precision without difficulty. A single measurement cycle needs about 20 seconds. A commercial GQMS system could be configured for high reliability using multiple units. The complete cost of such a system is about $250K. Figure 9 gives a schematic diagram of a possible GQMS system. The diagram shows a system with 4 equivalent sampling lines. By using two independent sets of electronics each servicing two mass spectrometers, we obtain a high probability of having at least one operational unit always. The overall size is modest. The electronics plus computer would occupy about 2' x 3' x 3' . The four GQMS's and sampling system would need a similar space. The GQMS section would need to be located near the gas flow being sampled. The control console could be hundreds of feet away if necessary. Automated operation could be achieved follow procedures we use for conventional noble gas mass spectrometry.

The point at which to sample the gas depends on the operation of the plant. Generally, being farther down the cleanup line is convenient since the GQMS has less to be protected from. The potential disadvantage would be the extent to which turbulent dispersion occurs. If a single pulse of gas were dispersed such that the gas appeared at the mass spectrometer over a long period, this would complicate the identification of the gas from individual assemblies. This dispersion can be measured in several ways; the noble gas tracers, ^{78}Kr and ^{124}Xe could be used.

For total isotope dilution measurements, the requirements on the mass spectrometer are much greater; low scattering, a large dynamic range for ion detection with high sensitivity for the minor isotopes (^{78}Kr, ^{124}Xe; for example). These requirement surpass the current commercial state-of-the-art. So it may be appropriate to consider using noble gas tracers such as ^{78}Kr and ^{124}Xe only occasionally and sending the samples to an outside laboratory. This could be a technique for testing the ventilation of the facility and supplying a calibration of the gas sampling system (i.e. introduce a known quantity of ^{124}Xe and see how much ends up in a set of samples).

Conclusions

Because of the ease of collection and measurement, the noble gas fission products could play an important role in reprocessing diagnostics. Diagnostics based on neutron capture probably have limited accuracy (5% ?) because of some combination of: 1) Kr and Xe redistribution, 2) need for detailed nuclear modeling. Diagnostics based on measuring total ^{86}Kr and ^{134}Xe have the potential for higher accuracy (1-2% perhaps). However, the increased analytical requirements for total isotope dilution will limit its application.

The on-line measurement of fission Kr and Xe could be done using commercially available hardware with custom computer software. The system would seek reliability by using multiple units and combining both gas mass spectrometry and gamma ray spectrometer (of ^{85}Kr). The cost to buy and assemble such a system is about $250,000 given 1993 prices (this does not include development engineering costs). The system would be completely automated and would need little maintenance.

Future research should be directed in four areas:

1) The radial distribution of fission Kr and Xe could be measured in a variety of representative fuel samples. This would determine how large the redistribution effect is and how regular is the process (i.e., does 95% of the Kr and Xe always reside in the outer 1/3 of the fuel?). The knowledge of the location of the Kr and Xe is important for the nuclear modeling of the system.

2) We want to understand better whether noble gas tracers can be used to determine total noble gas fission product abundances. This would focus on the abundances of the rare Kr and Xe isotopes and try to determine if they are derived strictly from air Kr and Xe additions to the sample. It is necessary to show that the light isotopes ^{78}Kr and ^{124}Xe come only from contributions of air Kr and Xe. Also, we need other isotopes that are strictly air derived. This set might include ^{126}Xe, ^{128}Xe, ^{129}Xe and ^{80}Kr since other Kr and Xe isotopes have important contributions from fission of neutron capture. An interesting by-product of these measurements will be data for ^{82}Kr and ^{130}Xe which are mainly produced by neutron captures on ^{81}Br and ^{129}I.

Since these isotopes are produced mainly by neutron capture and have only small fission contributions they are more sensitive than either ^{131}Xe or ^{83}Kr to neutron capture effects. In the context of the simple model presented, the ratio of ^{130}Xe to $^{131}Xe + ^{132}Xe$ is twice as sensitive as $^{132}Xe/^{131}Xe$ to neutron capture. If modeling is more important to the reduction of uncertainties, then the addition of data for ^{130}Xe and ^{82}Kr will add important constraints on the neutron energy spectrum and the overall balance of reactions.

3) We need to develop a sound method of modeling the data. It seems likely that the measurement of several isotopes each of Kr and Xe could independently constrain the modeling. That is, we could calculate burnup and Pu from only the Kr and Xe data. The most immediate goal is to determine what physical factors are most important. We know that the neutron energy spectrum and the initial ^{235}U enrichment are factors. Are there others and how can we express their general effects so that a parametrized model based on observed quantities can be constructed?

4) It would be desirable to conduct additional measurements of Kr and Xe from fuel dissolutions. These measurements are simple. The major question to be examined is, are the unusual problems associated with the collection and analysis of Kr. Why do the Kr isotopes seem to vary more than the Xe isotopes?

References

1) BENCHMARK, Reference data on post irradiation analysis of light water reactor fuel samples, 1983, S. Guardini and G. Guzzi, EUR 7879 EN, Commission of the European Communities, Nuclear Science and Technology.

2) The isotope correlation experiment, 1983, L. Koch and S. Schoof, EUR 7766 EN, Commission of the European Communities, Nuclear Science and Technology.

3) Gaseous isotope correlation technique for safeguards at reprocessing facilities, 1988, Michiaki Ohkubo, IAEA STR-240.

4) Balance and behavior of gaseous radionuclides released during initial PWR fuel reprocessing operations, 1983, A.Leudet, P.Miquel, P.J.Goumondy, G.Charrier, Proceedings of the 17th DOE Nuclear Air Cleaning Conference, p. 40-50.

5) Comportement des radionucleides gazeux degages pendant les operations initiales du retraitement, 1982, A.Leudet, A.Leseur, EUR 7322 FR Sciences et Techniques Nucleaires.

6) Personal communication, I. El Osery, 1992. The ORIGEN 2 calculation is for a PWR with standard initial uranium enrichment. The calculation was generated by V.Bragin in July,1992.

7) Nuclides and Isotopes 14th ed, 1989, F.W.Walker, J.R.Parrington, F.Feiner, General Electric Co.

8) Nuclear Power Technology -Vol. 2 - Fuel Cycle, 1983, p 175-180, ed. W.Marshall, Clarendon Press

Figure captions

Figure 1.

Graph of isotope ratios insensitive to neutron capture. The ratios change only a small amount because of burnup. The solid dots are from a calculation for a PWR using ORIGEN 2 (6). The burnup for the calculated points ranges from 5 to 30 GWd/tU. One point (from the second obrigheim set) does not plot on this scale. There is no explanation why the data from the first obrigheim set are so far to the right with respect to the other data and the ORIGEN 2 calculation.

Figure 2.

Graph of $^{132}Xe/^{131}Xe$ versus burnup as measured by ^{148}Nd. The solid dots are from the same ORIGEN 2 calculation as used in fig. 1. It is important to notice both the general linear trend and the deviations from it. The slope of the data matches the calculation. Variable deviations from the trend are seen within individual data sets.

Figure 3.

Graph of $^{84}Kr/^{83}Kr$ versus burnup as measured by ^{148}Nd. The solid dots are from the same ORIGEN 2 calculation as fig. 1. The overall deviation from the curve is greater than observed in fig. 2.

Figure 4.

Graph of $^{84}Kr/^{83}Kr$ versus $^{132}Xe/^{131}Xe$. In this graph we remove the reference to ^{148}Nd. We see that the noble gas indicators disagree with each other as much as with ^{148}Nd.

Figure 5.

Graph of $^{84}Kr/^{83}Kr$ versus $^{132}Xe/^{131}Xe$. The trajectory of the simple model is illustrated. For a specified initial ^{235}U enrichment, one can find a ratio of the neutron groups (spectral variable) and a burnup value that will exactly match the point on the graph. The spectral variable is determined by the data.

Figure 6.

Graph of burnup as measured by the simple model versus burnup given by ^{148}Nd. The overall agreement is a little better than for the global correlations seen in figs. 2 and 3. This improvement is expected because we now consider both the enrichment of uranium and the variations in neutron resonance captures. The figure does not include the Obrighiem data from either refs. 1 or 2, because of the variation seen in figure 1.

Figure 7.

Graph of ^{239}Pu by the model versus measured ^{239}Pu. The simple model can predict ^{239}Pu somewhat although that was not its principal task.

Figure 8.

Graph of $^{84}Kr/^{83}Kr$ versus $^{132}Xe/^{131}Xe$. The data show the composition of the Kr and Xe released on opening the sample, chopping the sample, and dissolving the sample. The ORIGEN 2 calculation is also shown. The Xe measurements group tightly with the sample type whereas the Kr measurements do not. The cause for this is not obvious.

Figure 9.

Schematic of a fission noble gas analysis system. Only half of the system is shown for clarity. The system has four sampling lines, two gamma ray spectrometers, four GQMS, two control units and two computers. The gas sampling system can switch from the process flow to a standard gas cylinder for calibration and performance verification.

Table 1. Summary of literature Kr and Xe isotopic compositions and fuel parameters

sample	% 235U	131Xe/ 134Xe	132Xe/ 134Xe	136Xe/ 134Xe	132Xe/ 131Xe	83Kr/ 86Kr	84Kr/ 86Kr	85Kr/ 86Kr	84Kr/ 83Kr	MWd/tU
				obrigheim I (PWR)						
86	3.10%	0.308	0.702	1.468	2.282					28974
87	3.10%	0.281	0.725	1.525	2.579	0.241	0.671		2.780	30917
88	3.10%	0.302	0.746	1.537	2.473	0.243	0.655		2.698	28895
89	3.10%	0.287	0.704	1.534	2.458	0.239	0.636		2.656	29671
90	3.10%	0.292	0.720	1.521	2.463	0.241	0.663		2.751	30181
91	3.10%	0.297	0.714	1.506	2.402	0.231	0.634		2.751	28542
92	3.10%	0.304	0.710	1.484	2.336	0.245	0.646		2.637	27061
93	3.10%	0.297	0.737	1.541	2.480	0.243	0.658		2.707	29857
94	3.10%	0.309	0.706	1.482	2.288	0.252	0.643		2.551	26452
95	3.10%	0.302	0.715	1.498	2.372	0.241	0.639		2.647	28650
				garigliano I (BWR)						
a1	1.60%	0.354	0.668	1.431	1.887	0.263	0.576	0.118	2.190	10590
a9	1.60%	0.339	0.682	1.517	2.012	0.245	0.590	0.114	2.408	14040
b1	1.60%	0.351	0.665	1.423	1.895	0.269	0.592	0.116	2.201	9800
j1	1.60%	0.342	0.682	1.481	1.994	0.257	0.596	0.116	2.319	12830
j9	1.60%	0.337	0.686	1.538	2.036	0.248	0.597	0.118	2.407	14480

Table 1. Summary of Kr and Xe isotopic compositions and fuel parameters (con't)

sample	% 235U	131Xe/ 134Xe	132Xe/ 134Xe	136Xe/ 134Xe	132Xe/ 131Xe	83Kr/ 86Kr	84Kr/ 86Kr	85Kr/ 86Kr	84Kr/ 83Kr	MWd/tU
				garigliano II (BWR)						
a3	2.10%	0.349	0.650	1.371	1.862	0.263	0.567	0.115	2.156	10510
b2	2.10%	0.351	0.655	1.358	1.866	0.268	0.570	0.117	2.127	10280
b8	2.10%	0.343	0.661	1.413	1.927	0.256	0.571	0.114	2.230	12150
c1	2.10%	0.349	0.653	1.368	1.871	0.264	0.567	0.111	2.148	10660
c3	2.10%	0.349	0.652	1.304	1.868	0.271	0.569	0.119	2.100	9140
d2	2.10%	0.349	0.652	1.327	1.868	0.270	0.568	0.110	2.104	9440
d4	2.10%	0.349	0.679	1.294	1.946	0.270	0.565	0.118	2.093	8850
e1	2.10%	0.348	0.657	1.364	1.888	0.265	0.573	0.112	2.162	10800
e5	2.10%	0.346	0.655	1.367	1.893	0.263	0.568	0.115	2.160	8930
g7	2.10%	0.349	0.659	1.349	1.888	0.270	0.570	0.118	2.111	10540
h2	2.10%	0.342	0.661	1.398	1.933	0.260	0.568	0.114	2.185	11920
h8	2.10%	0.347	0.667	1.404	1.922	0.262	0.586	0.119	2.237	12700

Table 1. Summary of Kr and Xe isotopic compositions and fuel parameters (con't)

sample	% 235U	131Xe/ 134Xe	132Xe/ 134Xe	136Xe/ 134Xe	132Xe/ 131Xe	83Kr/ 86Kr	84Kr/ 86Kr	85Kr/ 86Kr	84Kr/ 83Kr	MWd/tU
				trino I (PWR)						
I5 4	2.72%	0.328	0.662	1.406	2.018	0.257	0.564	0.095	2.195	14080
I5 9	2.72%	0.341	0.639	1.351	1.874	0.267	0.566	0.108	2.120	10070
j8 7	2.72%	0.329	0.666	1.429	2.024	0.255	0.563	0.104	2.208	14980
j8 9	2.72%	0.342	0.639	1.366	1.868	0.261	0.556	0.106	2.130	11000
a1 1	2.72%	0.352	0.617	1.295	1.753	0.267	0.548	0.108	2.052	8230
a1 7	2.72%	0.324	0.666	1.448	2.056	0.255	0.572	0.105	2.243	15290
h9 4	3.13%	0.325	0.666	1.403	2.049	0.255	0.565	0.106	2.216	16320
m11 7	3.90%	0.339	0.633	1.280	1.867	0.266	0.552	0.105	2.075	11920
				trino II (PWR)						
e5 7	3.13%	0.296	0.700	1.411	2.365	0.246	0.588		2.390	24220
e11 2	3.13%	0.311	0.694	1.362	2.232	0.252	0.578		2.294	20380
e11 4	3.13%	0.306	0.709	1.392	2.317	0.259	0.595		2.297	23450
e11 7	3.13%	0.300	0.709	1.399	2.363	0.246	0.588		2.390	24010
e11 8	3.13%	0.305	0.708	1.383	2.321	0.248	0.586		2.363	23150
e11 9	3.13%	0.319	0.684	1.340	2.144	0.253	0.575		2.273	19050
I11 4	3.13%	0.300	0.707	1.389	2.357	0.248	0.588		2.371	23650
I11 7	3.13%	0.301	0.711	1.396	2.362	0.246	0.587		2.386	24070
a1 7	3.13%	0.293	0.718	1.440	2.451	0.237	0.593		2.502	26550
j9 7	3.13%	0.300	0.713	1.406	2.377	0.244	0.591		2.422	24950

Table 1. Summary of Kr and Xe isotopic compositions and fuel parameters (con't)

sample	% 235U	131Xe/ 134Xe	132Xe/ 134Xe	136Xe/ 134Xe	132Xe/ 131Xe	83Kr/ 86Kr	84Kr/ 86Kr	85Kr/ 86Kr	84Kr/ 83Kr	MWd/tU
				obrighelm (PWR)						
d1 p1	3.00%	0.335	0.685	1.412	2.045					21170
e3 p2	3.00%	0.306	0.734	1.520	2.399	0.233	0.613	0.100	2.631	35100
e3 p4	3.00%	0.296	0.625	1.518	2.111	0.231	0.611	0.105	2.645	30920
g7 p1	3.00%	0.333	0.656	1.400	1.970	0.255	0.573	0.104	2.247	17130
g7 p3	3.00%	0.294	0.757	1.534	2.575	0.229	0.613	0.104	2.677	31320
g7 p5	3.00%	0.304	0.723	1.487	2.378	0.245	0.602	0.107	2.457	25810
m14 p1	3.00%	0.339	0.649	1.375	1.914	0.257	0.567	0.106	2.206	15600
m14 p4	3.00%	0.303	0.700	1.491	2.310	0.241	0.594	0.105	2.465	24900
g14 p31	2.83%	0.275	0.761	1.585	2.767	0.212	0.631	0.104	2.976	37490
k14 p41	2.83%	0.303	0.700	1.491	2.310	0.241	0.594	0.105	2.465	32900
				gundremmingen (BWR)						
b3	2.53%	0.303	0.698	1.424	2.304	0.245	0.589	0.107	2.404	21240
c5	2.53%	0.306	0.714	1.443	2.333	0.239	0.594	0.106	2.485	22970
e5	2.53%	0.294	0.711	1.510	2.418	0.258	0.581	0.121	2.252	25190
b3	2.53%	0.335	0.675	1.363	2.015	0.256	0.571	0.111	2.230	14390
c5	2.53%	0.327	0.666	1.404	2.037	0.254	0.573	0.111	2.256	15840
e5	2.53%	0.328	0.675	1.450	2.058	0.249	0.581	0.112	2.333	17490

Table 1. con't

		Borssele						
		total Kr (%)	82Kr (%)	83Kr (%)	84Kr (%)	85Kr (%)	86Kr (%)	MWd/tU
a8	open	0.70		11.48	31.00	5.67	51.86	31000
	chop	1.90		11.19	31.49	5.82	51.43	
	dissolve	97.40		11.42	31.06	5.81	51.62	
o6	open	1.20		11.10	31.60	5.30	52.00	31800
	chop	2.10						
	dissolve	96.70		11.78	31.01	6.02	51.03	
g15	open	3.80		11.71	30.71	5.58	52.00	31600
	chop	1.50	0.17	11.21	31.58	5.60	51.44	
	dissolve	94.70						
i15	open	4.50		11.88	30.78	5.50	51.84	31500
	chop	1.30	0.20	11.28	31.49	5.47	51.55	
	dissolve	94.20	0.22	11.65	31.00	5.52	51.61	
a10	open	2.20		11.67	30.83	5.57	51.92	31000
	chop	2.80	0.16	11.05	31.72	5.53	51.60	
	dissolve	95.00	0.15	11.60	31.02	5.53	51.77	

Table 1. con't

		Borssele							
		total Xe (%)	128Xe (%)	130Xe (%)	131Xe (%)	132Xe (%)	134Xe (%)	136Xe (%)	MWd/tU
a8	open	0.50		0.10	8.78	20.11	29.11	41.89	31000
	chop	1.70			7.50	21.24	28.42	42.83	
	dissolve	97.80		0.14	8.21	20.65	28.31	42.66	
o6	open	1.00			8.66	20.06	29.16	42.12	31800
	chop	1.80							
	dissolve	97.20			8.22	20.82	28.39	42.47	
g15	open	3.30		0.11	9.12	19.76	28.91	42.10	31600
	chop	1.30	0.04	0.15	7.60	21.16	28.18	42.92	
	dissolve	95.40			8.17	20.72	28.37	42.65	
i15	open	4.10	0.03	0.11	9.10	19.66	28.89	42.21	31500
	chop	1:00	0.05	0.18	7.59	21.12	28.18	42.86	
	dissolve	94.90	0.04	0.14	8.14	20.54	28.36	42.81	
a10	open	1.90		0.10	9.02	19.80	29.06	42.02	31000
	chop	2.40	0.04	0.15	7.40	21.20	28.14	42.75	
	dissolve	95.70		0.15	8.13	20.65	28.34	42.81	

Table 2. Correlation of 132Xe/131Xe with burnup

sample ID	MWd/tU (Nd)	132Xe/131Xe	MWd/tU (predicted)	deviation
86	28974	2.282	23527	-18.8%
87	30917	2.579	32659	5.6%
88	28895	2.473	29396	1.7%
89	29671	2.458	28939	-2.5%
90	30181	2.463	29107	-3.6%
91	28542	2.402	27223	-4.6%
92	27061	2.336	25199	-6.9%
93	29857	2.480	29606	-0.8%
94	26452	2.288	23724	-10.3%
95	28650	2.372	26313	-8.2%
a1	10590	1.887	11399	7.6%
a9	14040	2.012	15233	8.5%
b1	9800	1.895	11632	18.7%
j1	12830	1.994	14691	14.5%
j9	14480	2.036	15964	10.3%
a3	10510	1.862	10645	1.3%
b2	10280	1.866	10757	4.6%
b8	12150	1.927	12631	4.0%
c1	10660	1.871	10909	2.3%
c3	9140	1.868	10821	18.4%
d2	9440	1.868	10821	14.6%
e1	10800	1.888	11427	5.8%
g7	10540	1.888	11437	8.5%
h2	11920	1.933	12804	7.4%
h8	12700	1.922	12480	-1.7%
l5 4	14080	2.018	15432	9.6%
l5 9	10070	1.874	10996	9.2%
j8 7	14980	2.024	15617	4.3%
j8 9	11000	1.868	10828	-1.6%
a1 1	8230	1.753	7277	-11.6%
a1 7	15290	2.056	16577	8.4%

Table 2. Correlation of 132Xe/131Xe with burnup (con't)

sample ID	MWd/tU (Nd)	132Xe/131Xe	MWd/tU (predicted)	deviation
h9 4	16320	2.049	16383	0.4%
m11 7	11920	1.867	10792	-9.5%
e5 7	24220	2.365	26080	7.7%
e11 2	20380	2.232	21983	7.9%
e11 4	23450	2.317	24609	4.9%
e11 7	24010	2.363	26033	8.4%
e11 8	23150	2.321	24742	6.9%
e11 9	19050	2.144	19301	1.3%
l11 4	23650	2.357	25828	9.2%
l11 7	24070	2.362	25996	8.0%
a1 7	26550	2.451	28711	8.1%
j9 7	24950	2.377	26442	6.0%
d1 p1	21170	2.045	16246	-23.3%
e3 p2	35100	2.399	27119	-22.7%
g7 p1	17130	1.970	13948	-18.6%
g7 p3	31320	2.575	32530	3.9%
g7 p5	25810	2.378	26492	2.6%
m14 p1	15600	1.914	12242	-21.5%
m14 p4	24900	2.310	24401	-2.0%
g14 p31	37490	2.767	38443	2.5%
b3	21240	2.304	24199	13.9%
c5	22970	2.333	25111	9.3%
e5	25190	2.418	27724	10.1%
b3	14390	2.015	15329	6.5%
c5	15840	2.037	15998	1.0%
e5	17490	2.058	16650	-4.8%
u235 th	0	1.489		
Points not included in the regression analysis				
e3 p4	30920	2.111	18296	-40.8%
d4	8850	1.946	13198	49.1%
e5	8930	1.893	11585	29.7%
k14 p41	32900	2.310	24401	-25.8%

Table 3. Correlation of 84Kr/83Kr with burnup

sample ID	MWd/tU (Nd)	84Kr/83Kr	MWd/tU (predicted)	deviation
87	30917	2.780	34023	10.0%
88	28895	2.698	31169	7.9%
89	29671	2.656	29709	0.1%
90	30181	2.751	32997	9.3%
91	28542	2.751	32994	15.6%
92	27061	2.637	29060	7.4%
93	29857	2.707	31492	5.5%
94	26452	2.551	26051	-1.5%
95	28650	2.647	29410	2.7%
a1	10590	2.190	13520	27.7%
b1	9800	2.201	13889	41.7%
j1	12830	2.319	18000	40.3%
a3	10510	2.156	12331	17.3%
b2	10280	2.127	11322	10.1%
b8	12150	2.230	14922	22.8%
c1	10660	2.148	12047	13.0%
c3	9140	2.100	10376	13.5%
d2	9440	2.104	10518	11.4%
d4	8850	2.093	10132	14.5%
e1	10800	2.162	12552	16.2%
e5	8930	2.160	12463	39.6%
g7	10540	2.111	10775	2.2%
h2	11920	2.185	13329	11.8%
h8	12700	2.237	15136	19.2%
l5 4	14080	2.195	13674	-2.9%
l5 9	10070	2.120	11079	10.0%
j8 7	14980	2.208	14136	-5.6%
j8 9	11000	2.130	11441	4.0%
a1 1	8230	2.052	8736	6.2%
a1 7	15290	2.243	15362	0.5%

Table 3. Correlation of 84Kr/83Kr with burnup (con't)

sample ID	MWd/tU (Nd)	84Kr/83Kr	MWd/tU (predicted)	deviation
h9 4	16320	2.216	14408	-11.7%
m11 7	11920	2.075	9527	-20.1%
e5 7	24220	2.390	20473	-15.5%
e11 2	20380	2.294	17117	-16.0%
e11 4	23450	2.297	17244	-26.5%
e11 7	24010	2.390	20473	-14.7%
e11 8	23150	2.363	19523	-15.7%
e11 9	19050	2.273	16390	-14.0%
l11 4	23650	2.371	19803	-16.3%
l11 7	24070	2.386	20332	-15.5%
a1 7	26550	2.502	24359	-8.3%
j9 7	24950	2.422	21581	-13.5%
e3 p2	35100	2.631	28834	-17.9%
e3 p4	30920	2.645	29325	-5.2%
g7 p1	17130	2.247	15498	-9.5%
g7 p3	31320	2.677	30431	-2.8%
g7 p5	25810	2.457	22797	-11.7%
m14 p1	15600	2.206	14079	-9.7%
m14 p4	24900	2.465	23061	-7.4%
g14 p31	37490	2.976	40838	8.9%
b3	21240	2.404	20954	-1.3%
c5	22970	2.485	23777	3.5%
b3	14390	2.230	14922	3.7%
c5	15840	2.256	15806	-0.2%
e5	17490	2.333	18496	5.7%
u235 th	0	1.866	2248	

Points not included in the regression analysis

a9	14040	2.408	21095	50.3%
e5	25190	2.252	15668	-37.8%
j9	14480	2.407	21064	45.5%
k14 p41	32900	2.465	23061	-29.9%

Table 4. Comparison of Kr and Xe based burnup to Nd based burnup

	MWd/tU (Kr&Xe)	MWd/tU (Nd)	deviation (%)
	GARIGLIANO I		
d4	7883	8850	-10.9%
c3	8457	9140	-7.5%
d2	8625	9440	-8.6%
g7	8844	10540	-16.1%
h8	12746	12700	0.4%
b8	12588	12150	3.6%
h2	11329	11920	-5.0%
e5	10553	8930	18.2%
e1	10650	10800	-1.4%
a3	10473	10510	-0.4%
b2	9464	10280	-7.9%
c1	10192	10660	-4.4%
	GARIGLIANO II		
j9	13137	14480	-9.3%
a1	8602	10590	-18.8%
a9	13005	14040	-7.4%
j1	11522	12830	-10.2%
b1	8880	9800	-9.4%

Table 4. Comparison of Kr and Xe .... (con't)

	MWd/tU (Kr&Xe)	MWd/tU (Nd)	deviation (%)
	TRINO I		
a1,1	9745	8230	18.4%
a1,7	16724	15290	9.4%
j8,9	12774	11000	16.1%
j8,7	15480	14980	3.3%
l5,4	14974	14080	6.4%
l5,9	12286	10070	22.0%
m11,7	15080	11920	26.5%
h9,4	18077	16320	10.8%
	TRINO II		
a1,7	27003	26550	1.7%
j9,7	24889	24950	-0.2%
e11,2	20792	20380	2.0%
e11,4	20835	23450	-11.2%
e11,7	23939	24010	-0.3%
e11,8	23106	23150	-0.2%
e11,9	20137	19050	5.7%
l11,4	23359	23650	-1.2%
l11,7	23838	24070	-1.0%
e5,7	23939	24220	-1.2%

Table 4. Comparison of Kr and Xe .... (con't)

	MWd/tU (Kr&Xe)	MWd/tU (Nd)	deviation (%)
	OBRIGHEIM		
e2p2	28549	35100	-18.7%
e3p4	27910	30920	-9.7%
g7p1	17310	17130	1.1%
g7p3	29742	31320	-5.0%
g7p5	24916	25810	-3.5%
m14p1	17268	15600	10.7%
m14p4	24887	24900	-0.1%
g14p3 1	32986	37490	-12.0%
k14p4 1	23726	32900	-27.9%
	GUNDREMMINGEN		
b b3	20289	21240	-4.5%
b c5	22059	22970	-4.0%
b e5	25028	25190	-0.6%
c b3	15187	14390	5.5%
c c5	15980	15840	0.9%
c e5	18186	17490	4.0%

Fig. 1. Graph of quantities relatively insensitive to neutron capture

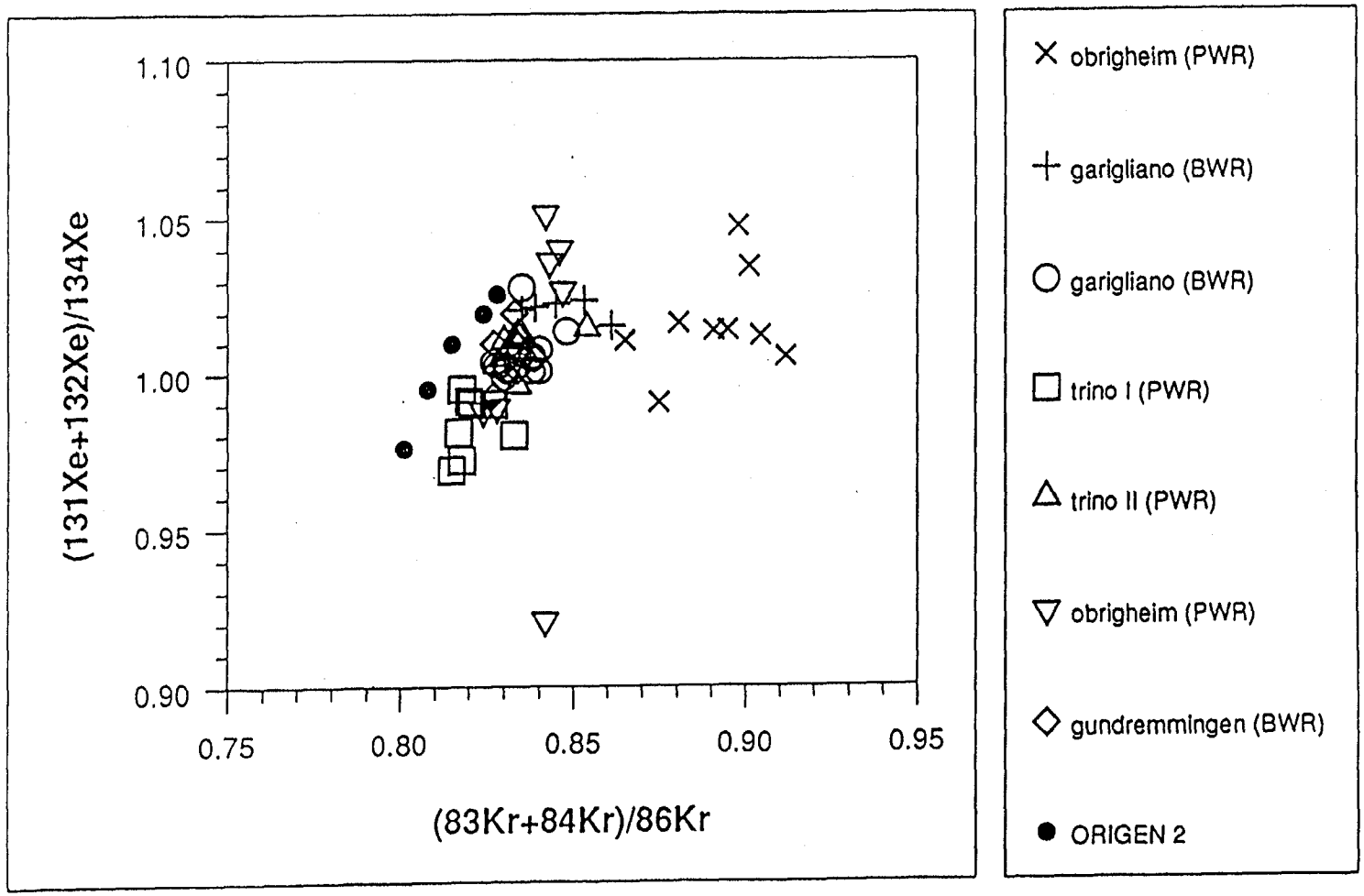

Fig. 2. Correlation between 132Xe/131Xe and burnup

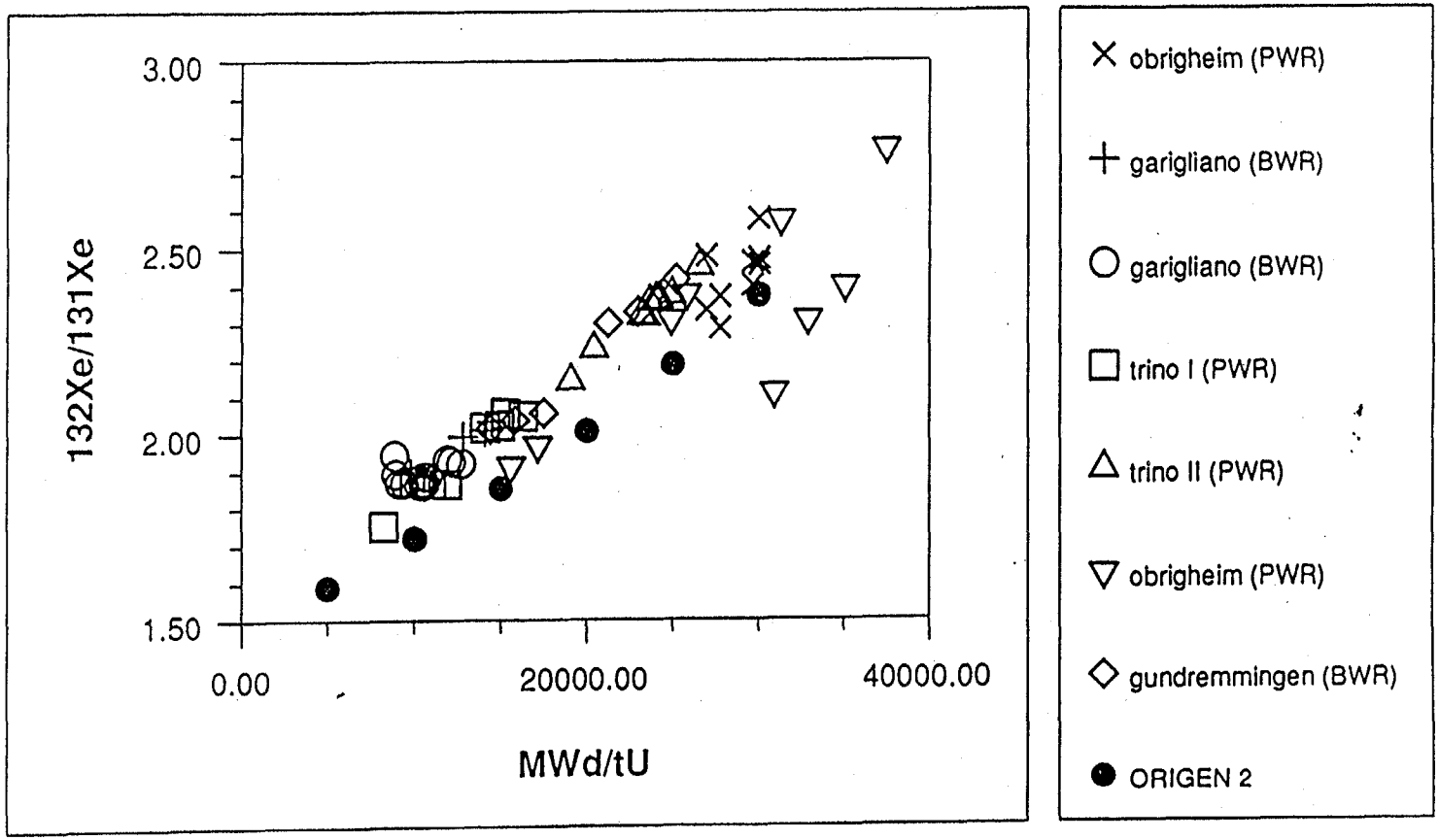

Fig. 3 Correlation between 84Kr/83Kr and burnup

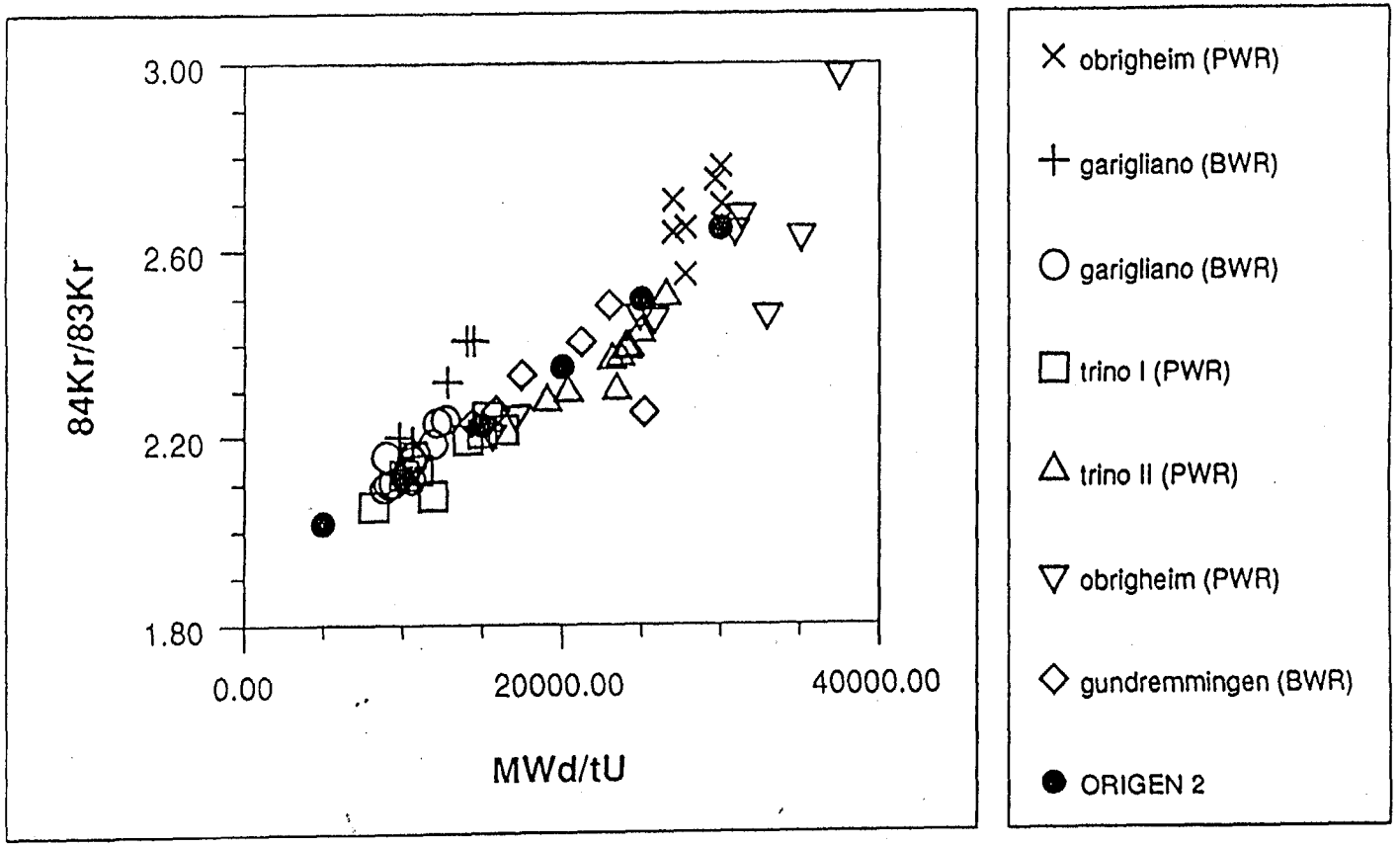

Fig. 4 Correlation between 84Kr/83Kr and 132Xe/131Xe

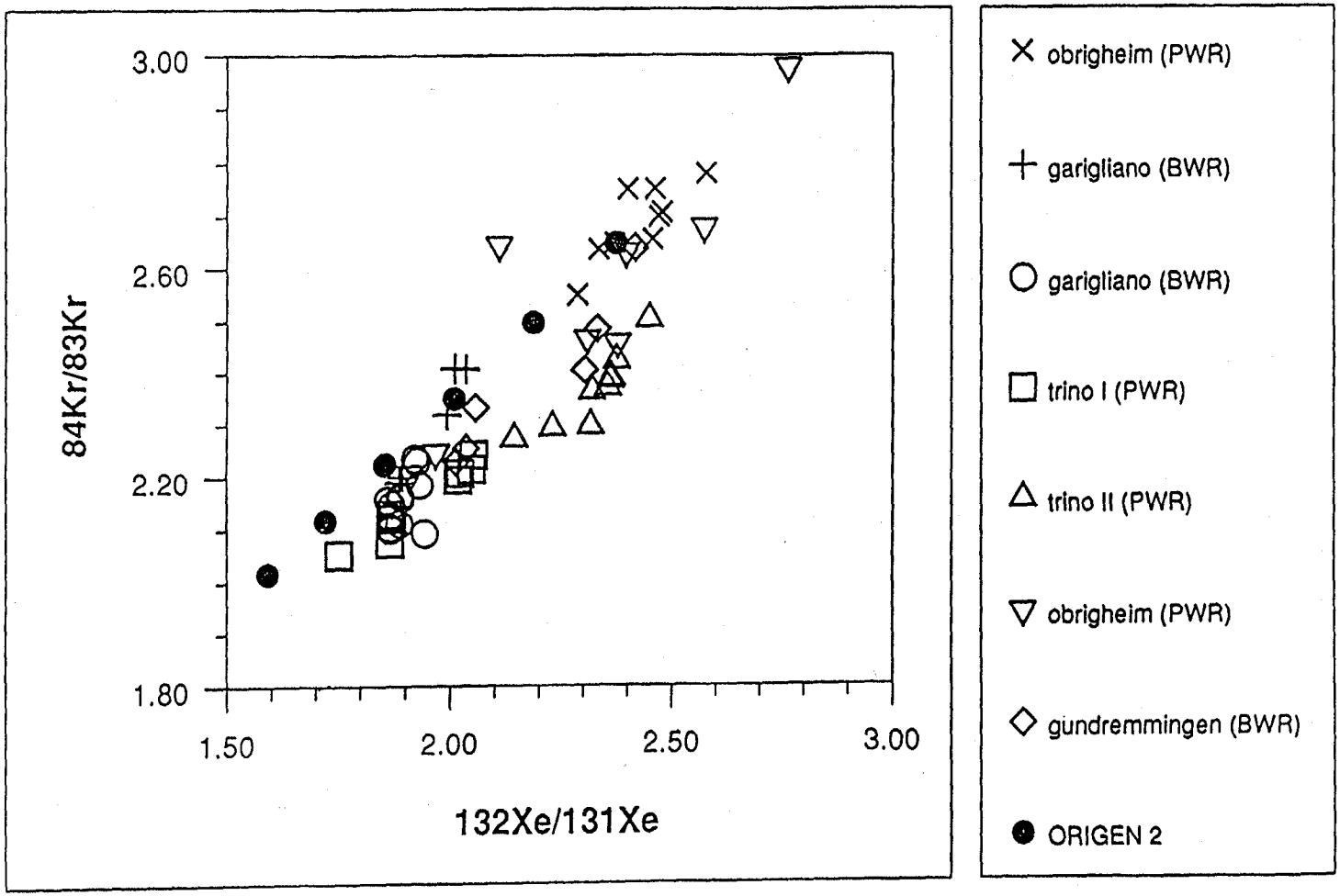

Fig. 5. Example of a model calculation to match observed Kr and Xe data

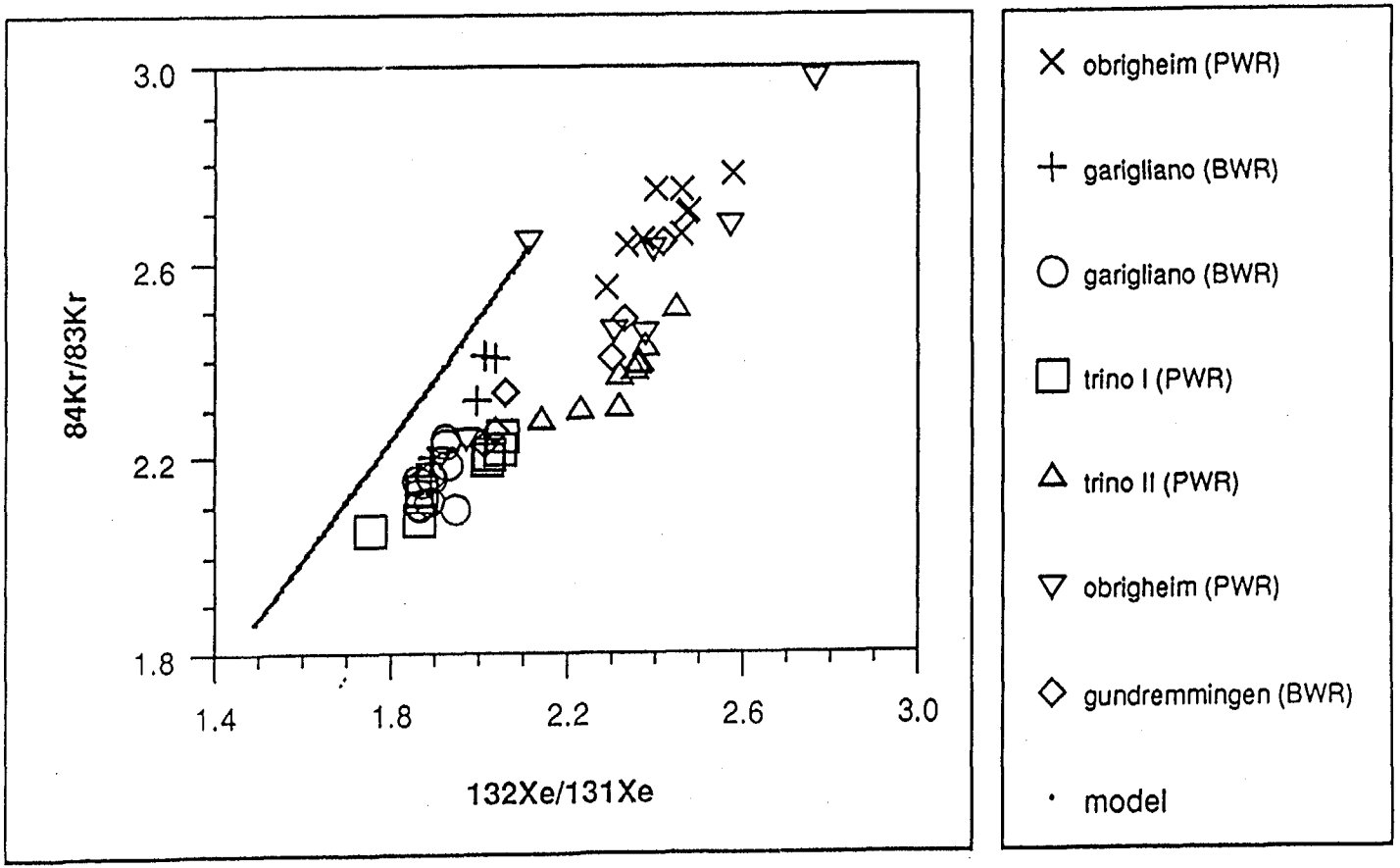

Fig. 6. Comparison of measured burnup and burnup calculated from the simple model and Kr and Xe data

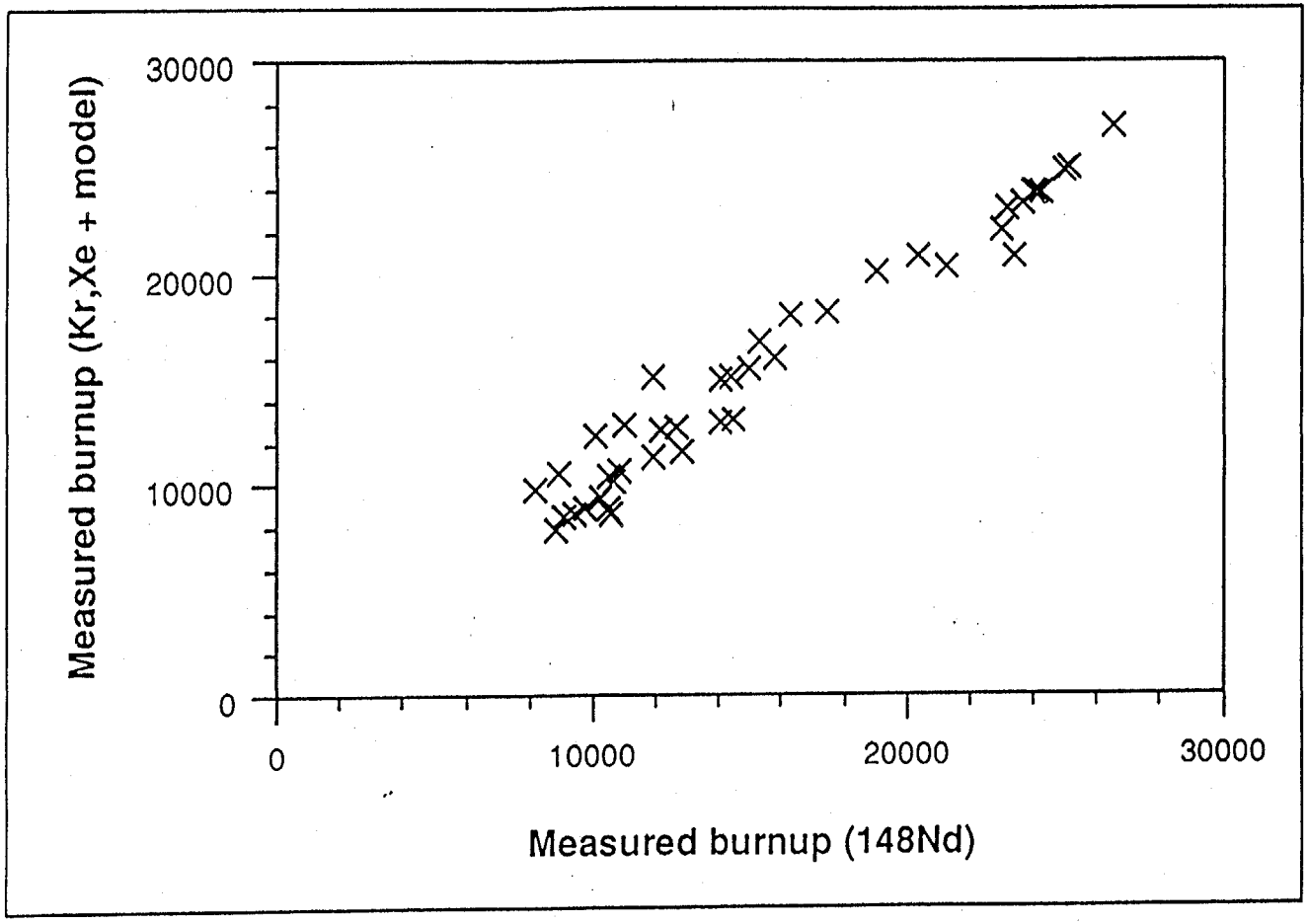

Fig. 7. Comparison of measured 239Pu and 239Pu calculated from the simple model

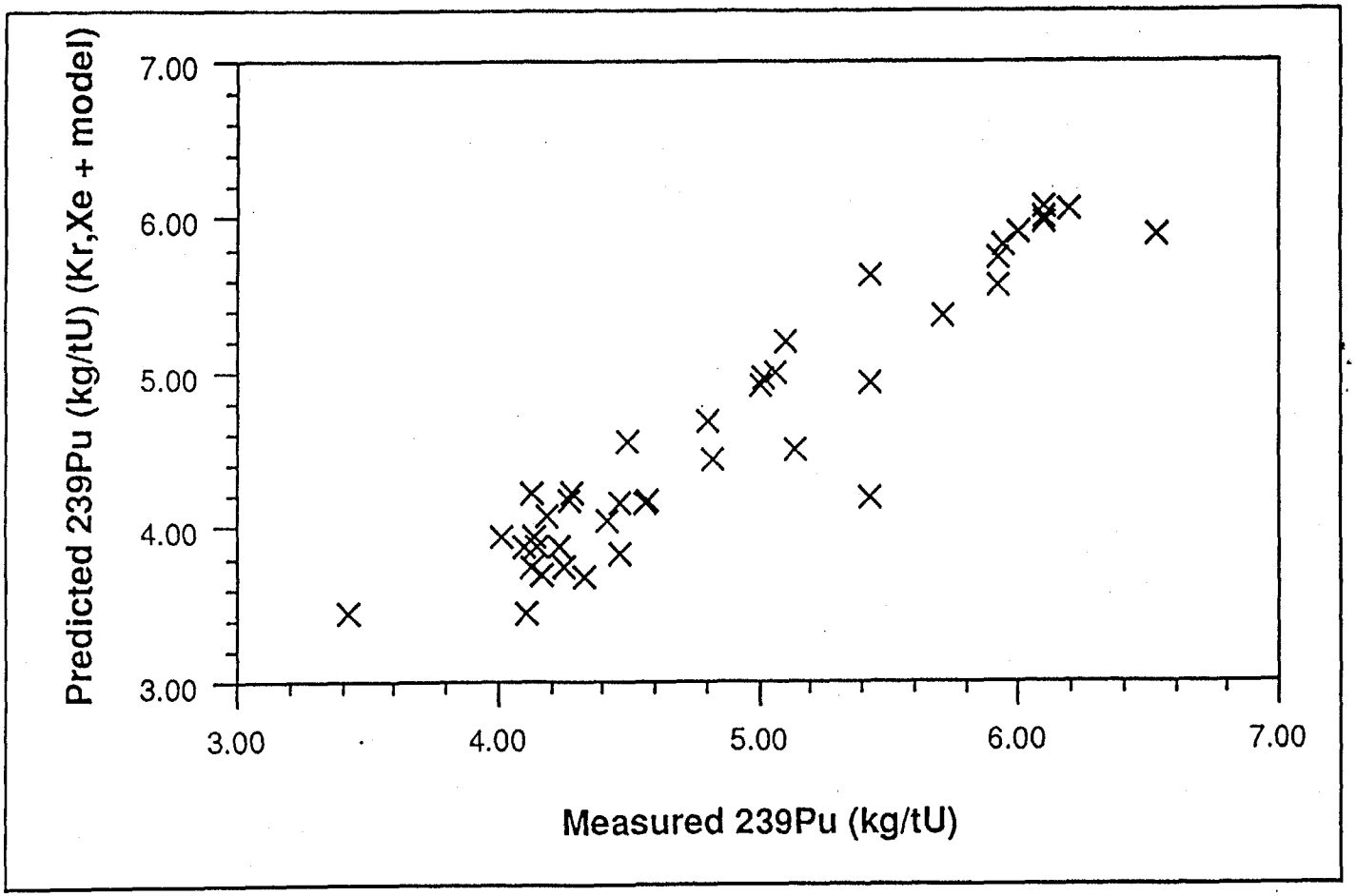

Fig. 8. Graph of 84Kr/83Kr versus 132Xe/131Xe for samples from the Borsseile reactor

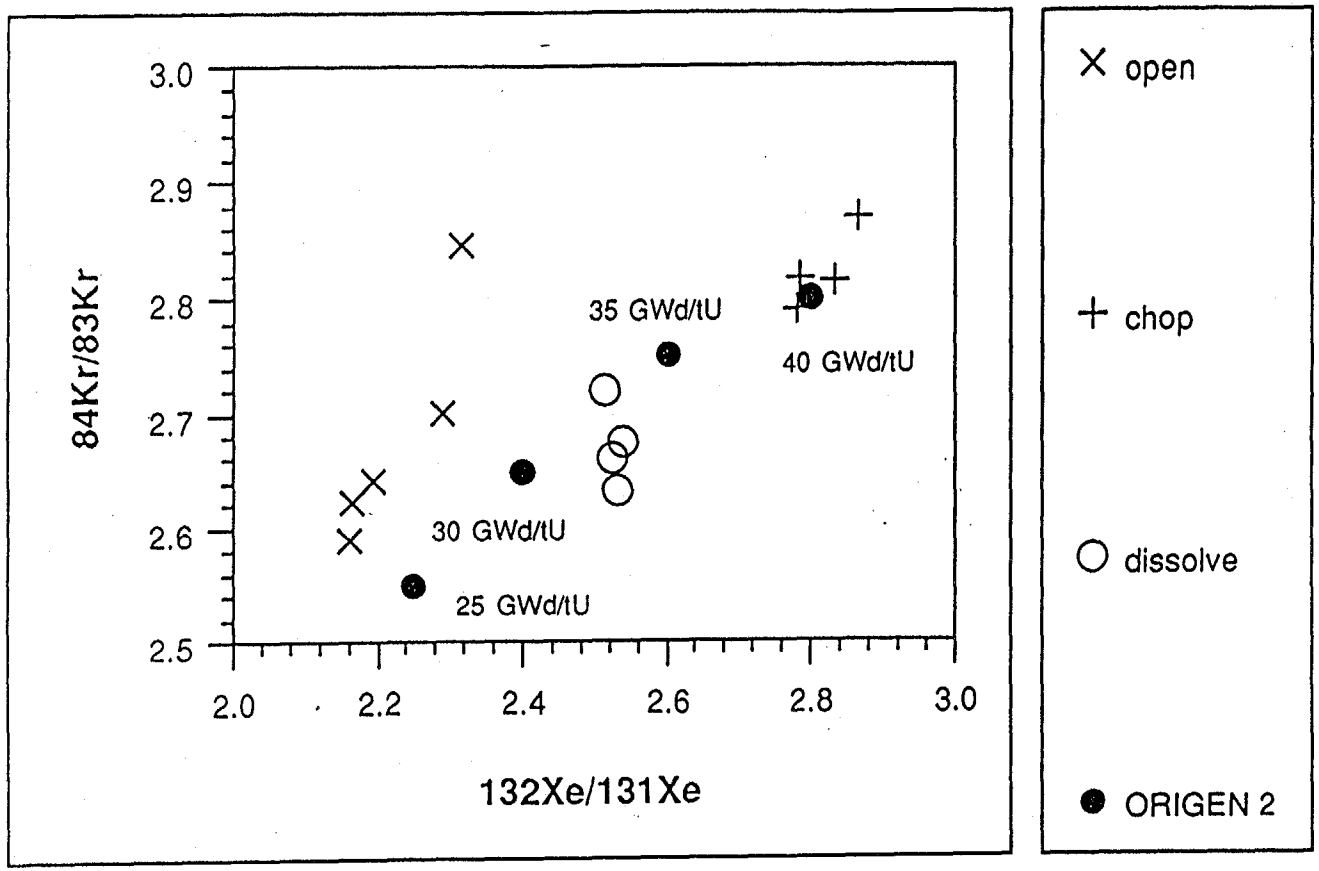

Fig. 9. Schematic of 1/2 of the proposed QMS noble gas analysis system